

## Numerical Modelling of Conventional and Incremental Forming of Thin-Walled Tube

Carlos Suntaxi<sup>1,2,a\*</sup>, Gabriel Centeno<sup>1,b</sup>, Ana Rosa-Sainz<sup>1,c</sup>,  
Domingo Morales-Palma<sup>1,d</sup> and Carpóforo Vallellano<sup>1,e</sup>

<sup>1</sup>Department of Mechanical and Manufacturing Engineering, University of Seville, Spain

<sup>2</sup>Departament of Mechanical Engineering, Escuela Politécnica Nacional, Quito, Ecuador

<sup>a</sup>segundo.suntaxi@epn.edu.ec, <sup>b</sup>gaceba@us.es, <sup>c</sup>arosa@us.es, <sup>d</sup>dmpalma@us.es,  
<sup>e</sup>carpofofor@us.es

**Keywords:** Tube forming, incremental forming, formability, failure, fracture

**Abstract.** This study presents a numerical analysis of the tube expansion process by conventional tube-end forming versus single point incremental forming (SPIF) using DEFORM. The work includes the assessment of the strain paths within the principal strain space of these processes with respect to the formability limits as well as their evaluation within the equivalent strain versus stress triaxiality space. The results obtained demonstrated that the mechanics of tube flaring process in conventional and incremental forming are substantially different. This analysis of formability in the light of the accumulated equivalent strain and the average stress triaxiality allowed a better understanding of the differences between both processes in terms of the fracture limit strains.

### Introduction

A series of papers starting with Centeno et al. [1] in 2016, in which formability and failure of tube-end expansion is assessed by means of circle grid analysis (CGA), aimed the establishment of plastic deformation processes for the combined determination of forming limits at necking and fracture for thin-walled tube. This work was followed by others using numerical methods in combination with digital image correlation (DIC) [2] and also utilizing others processes such as tube inversion [2] or internal bulging [3] for allowing the establishment of the material forming limit diagram (FLD) at necking and fracture for a range of strain paths corresponding to mode I of fracture mechanics, i.e. from uniaxial tension towards equi-biaxial strain with strain ratios ( $\beta$ ) between -1/2 and 1. Very recently, Magrinho et al. [4] evaluated the mode II fracture loci, i.e. the shear FFL or SFFL for tubes.

On the other hand, the metal forming community has had a great interest in incremental sheet forming (ISF) processes for the last few decades, especially due to the enhancement of formability attained in ISF, as discussed in the review paper by McAnulty et al. [5] for single point incremental forming (SPIF). In this sense, most of the research focusing in formability and failure in ISF/SPIF coincide in the fact that failure is attained by ductile fracture in the absence of necking [6,7]. Related to formability and failure in SPIF, a number of researchers have pointed out the non-proportionality of the plastic straining in incremental forming. In 2007, Eyckens et al. [8] predicted numerically non-monotonic serrated strain paths SPIF, claiming that this effect was related to the enhancement of formability above the material FLC. Following the assumption of non-proportional plastic straining in ISF, Mirnia and Shamsari [9] proposed a procedure for predicting failure in SPIF based in the utilization of the stress triaxiality. This allows establishing a strain path within the space of stress triaxiality versus equivalent strain, i.e. the so called triaxiality space, firstly used by Vujovic and Shabaik [10] and later generalized by the work of Wierzbicki and collaborators [11], which would be suitable for assessing the material failure especially in the case of non-proportional processes as ISF.

In this scientific context, and following the very recently published work by Suntaxi et al. [12], this paper aimed providing a novel perspective of formability and failure in the non-proportional process of multi-stage tube expansion by SPIF, discussing the validity of the conventional forming limits for incremental forming processes. The study was carried out by means of numerical modelling of the SPIF process combined with a numerical analysis of the strain paths within the equivalent strain

versus stress triaxiality space, including a comparison with conventional tube expansion. The results demonstrated the suitable use of the average stress triaxiality for assessing formability and failure in multi-stage tube expansion by SPIF as well as other incremental tube forming processes.

### Numerical Modelling

The numerical study made use of the commercial software DEFORM<sup>TM</sup>-3D, which adopts the flow formulation of the finite element method (FEM) for modelling the plastic deformation of the tube consequence of the different processes considered. The isotropic elastic and plastic tube material (AA6063-T6 tube of 2 mm thickness) behavior followed the experimental power law (see details in [1]). Mises plasticity model was set and no strain rate effects were considered due to the quasi-static plastic deformation of the process. bodies and discretized by means of spatial triangular elements. A penalty contact algorithm was used for modelling the dies-tube contact interfaces.

In the case of conventional expansion with a rigid punch, the numerical model used the rotational symmetry condition for creating a simplified numerical model of an angular sector of 18 degrees (i.e. 1/20 of the full model). Slightly more than 10,000 tetrahedrons were used with an initial average side length of 1 mm with a refinement to 0.25 mm in the tube edge. More details on this numerical modeling can be found in [12]. More details about the conventional expansion process and the corresponding strain paths can be found elsewhere [1,3].

In the case of the thin-walled tube expansion process by SPIF the initial tube was meshed using about 50,000 3D tetrahedrons including the 2 meshing zones considered. As depicted in Fig. 1a, the upper region (the tool-tube contact area) was characterized by elements with a smaller size in order to provide more accurate results. Automatic re-meshing was used (resulting in approximately 120,000 elements in the final step depicted in Fig. 1b) due to the high strain values reached during the multi-stage expansion by SPIF. The punch was modelled as a rigid body following the real trajectory of the punch defined in the experimental tests. The elements in the region in contact with the clamping device were pinned (as depicted in Fig. 1a). The process parameters of the experiments on multi-stage expansion by SPIF can be found in [12,13].

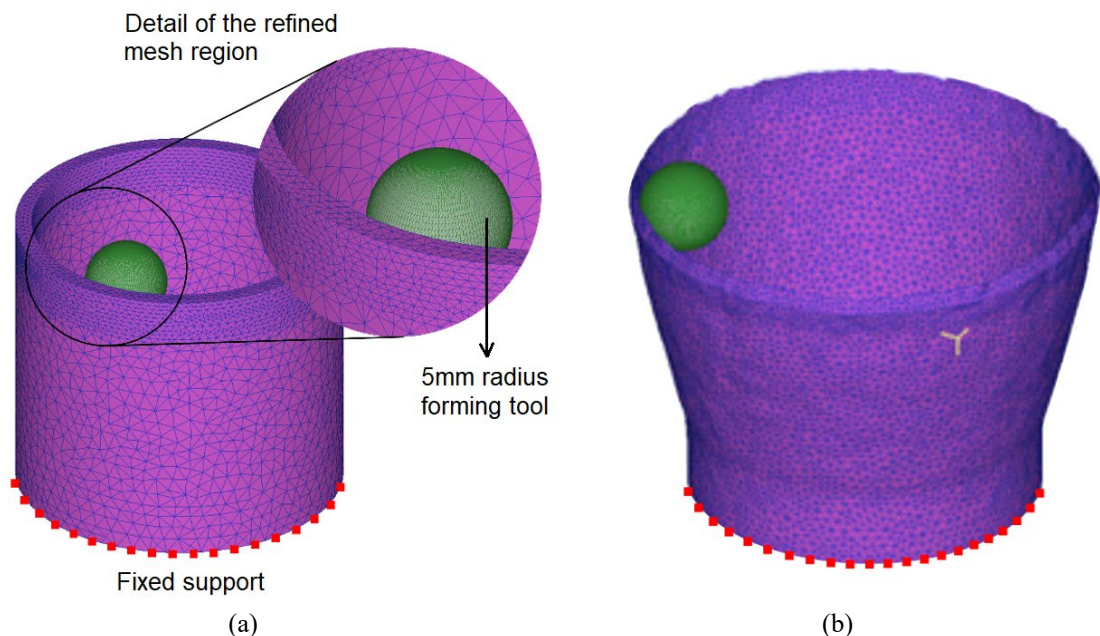


**Figure 1.** (a) Initial mesh of the tube including 2 meshing zones and boundary conditions and (b) deformed shaped of the final tube after 8 incremental forming stages

### Analytical Framework

As discussed in the previous research by the authors on SPIF of tubes [13], fracture is assumed to occurred principally by means of void growth in mode I of fracture mechanics (in-plane tension) following the unified vision of Martins et al. [14]. This vision makes use of the non-coupled damage criterion based on void growth presented by McClintock in [15] that was expressed by Atkins [16] into the damage function provided in Eq. 1.

$$D = \int \frac{\sigma_H}{\bar{\sigma}} d\bar{\varepsilon} \quad (1)$$

In Eq. 1, the mathematical function to be integrated, i.e. the ratio of the hydrostatic stress  $\sigma_H$  to the equivalent stress  $\bar{\sigma}$ , is defined in Eq. 2 as stress triaxiality  $\eta$ . Beyond the maximum level of strains attained in forming process, stress triaxiality has revealed to be one of the most important factors affecting formability, especially in a non-proportional forming process such as SPIF, as has been discuss for the case of incremental forming of sheet metals [7].

$$\eta = \frac{\sigma_H}{\bar{\sigma}} \quad (2)$$

In this context, assuming that loading was proportional in the formability tests for assessing the tube material FLD [3] and that the material is isotropic by means of the von Mises plasticity criterion, the transformation of the experimental strain loading path from the principal strain space to the space of effective (equivalent) strain versus stress triaxiality is carried out analytically by assuming the tube expansion to occur under plane stress deformation conditions ( $\sigma_t = \sigma_3 = 0$ ) in the thickness direction. Under these simplifying assumptions, the effective stress  $\bar{\sigma}$  and the increment of effective strain  $d\bar{\varepsilon}$  are expressed as follows in Eq. 3 and Eq. 4:

$$\bar{\sigma} = \sqrt{\sigma_1^2 - \sigma_1\sigma_2 + \sigma_2^2} \quad (3)$$

$$d\bar{\varepsilon} = \frac{2}{\sqrt{3}} \sqrt{d\varepsilon_1^2 + d\varepsilon_1 d\varepsilon_2 + d\varepsilon_2^2} \quad (4)$$

By applying the Levy–Mises constitutive equations as in [3], it is possible to write the effective strain  $\bar{\varepsilon}$  and stress-triaxiality  $\eta$  as a function of the slope  $\beta = d\varepsilon_2/d\varepsilon_1$  of the strain loading path as follows in Eq. 5 and in Eq. 6, respectively:

$$\bar{\varepsilon} = \frac{2}{\sqrt{3}} \sqrt{1 + \beta + \beta^2} \varepsilon_1 \quad (5)$$

$$\eta = \frac{1 + \beta}{\sqrt{3} \sqrt{1 + \beta + \beta^2}} \quad (6)$$

In addition to that, the kink of the strain path from necking strains towards fracture should be also considered in the transformation of the FFL, providing a more formal assessment of the fracture limit in physical terms. To this purpose, the resulting equations calculated in Martinez-Donaire et al. [17] are adapted for the case of von Mises plasticity ( $r=1$ ) resulting in Eq. 7 and Eq. 8.

$$\bar{\varepsilon}_f = \int_0^{\bar{\varepsilon}_n} d\bar{\varepsilon} + \int_{\bar{\varepsilon}_n}^{\bar{\varepsilon}_f} d\bar{\varepsilon} = \frac{2}{\sqrt{3}} \left[ \varepsilon_{1f} + \left( \sqrt{1 + \beta + \beta^2} - 1 \right) (\varepsilon_{2f}/\beta) \right] \quad (7)$$

$$\bar{\eta}_f = \frac{1}{\bar{\varepsilon}_f} \int_0^{\bar{\varepsilon}_f} \frac{\sigma_m}{\bar{\sigma}} d\bar{\varepsilon} = \frac{1}{\bar{\varepsilon}_f} \left( \int_0^{\bar{\varepsilon}_n} \frac{\sigma_m}{\bar{\sigma}} d\bar{\varepsilon} + \int_{\bar{\varepsilon}_n}^{\bar{\varepsilon}_f} \frac{\sigma_m}{\bar{\sigma}} d\bar{\varepsilon} \right) = \frac{\sqrt{3}}{3} \left[ \frac{\varepsilon_{1f} + \varepsilon_{2f}}{\varepsilon_{1f} + \left( \sqrt{1 + \beta + \beta^2} - 1 \right) (\varepsilon_{2f}/\beta)} \right] \quad (8)$$

As a consequence, the FLD within the principal strains space obtained in [3] is transformed into the space of triaxiality shown in Fig. 2, defined by the necking (FLC) and Fracture (FFL) limits, respectively. Notice that these limits differs to those calculated in Magrinho et al. [3] by considering Hosford's anisotropic criterion. In addition to that, notice that the FFL calculated considering the kink

of the strain path until fracture differs very slightly to that calculated with a constant value of  $\beta$ , as it was constructed in the cited previous research [3].

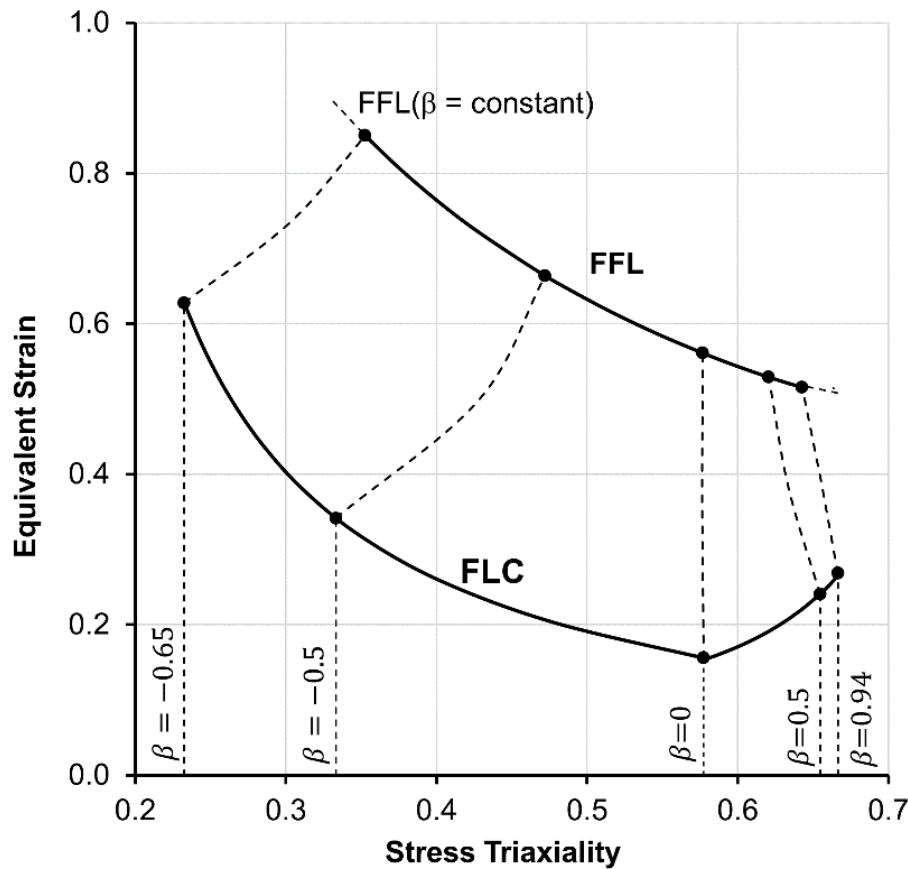


**Figure 2.** FLC and FFL of the tube material (assumed isotropic) within the triaxiality space considering the kink of the strain path in the transformation

Finally, it must be also pointed out that in this research the material was assumed to be isotropic because of a number of reasons: (i) the huge computational cost that would be greater in the case of considering anisotropy, (ii) the absent of the implementation of the Hosford's criterion in DEFORM, (iii) the difficulties for evaluating Lankford's coefficient at  $45^\circ$  for a tube, and (iv) the fair results obtained by assuming the tube to be isotropic in the previous paper by Cristino et al. [13].

## Results and Discussion

The numerical model is validated in terms of principal strains by comparing the results provided by the finite element modelling using DEFORM<sup>TM</sup>-3D with the experimental values of the CGA carried out using ARGUS<sup>®</sup>. As depicted in Fig. 3, this comparison is carried out along a section parallel to the tube axis and covering the region of homogeneous straining, i.e. where the tube thickness decreases as approaching the tube end. On the other hand, the section plotted on the numerical model of the expanded tool ends at the same precise point ("point A", see more details in [12] for the assessment of this point location), whereas the experimental strains contain the pairs of principal strains along 3 parallel sections up to the very tube edge. Finally, the pair of in-plane principal strains at fracture (red triangle in Fig. 3) was calculated as an average of the fracture strains of the different specimens tested following the procedure explain in [12]. This fracture strain is characterized by a value of  $\bar{\epsilon} = 1.17$  of equivalent strain that defines the Mises iso-equivalent fracture elliptical locus plotted in dotted line in Figure 3. This locus will be later used in the triaxiality analysis and is transformed into a horizontal limit in that space.

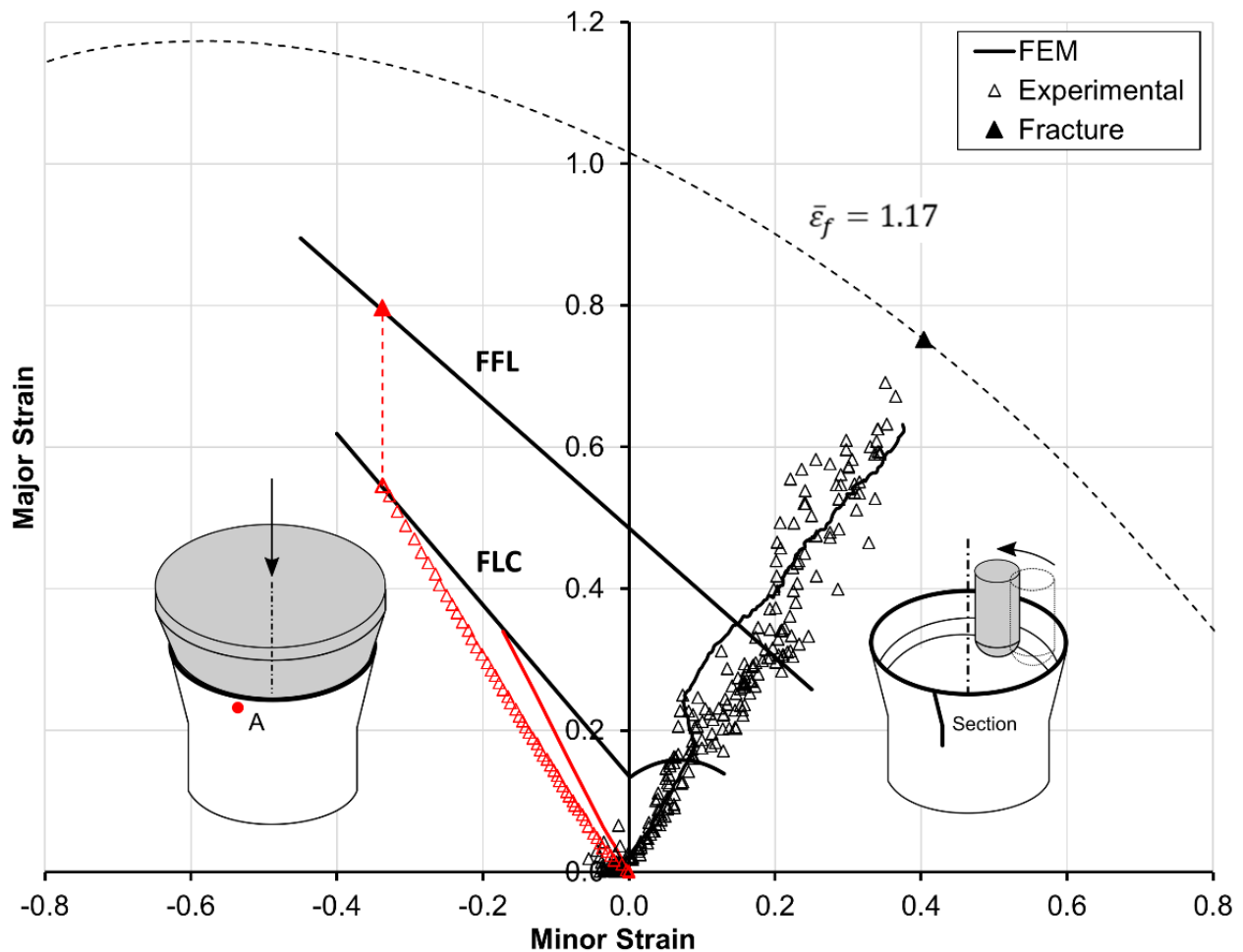


**Figure 3.** Experimental principal strains versus numerical predictions in conventional tube expansion versus multi-stage incremental tube expansion

As can be seen in Fig. 3, there exist a good agreement of the numerical with the experimental results, thus allowing to use the numerical model to provide accurate values of principal strains. Indeed, the numerical and experimental results are located in the same equi-biaxial region of the principal strain space with a similar evolution towards the principal strains at fracture as approaching the tube end. The small difference in the maximum level of strains, slightly below in the case of the numerical model, are a consequence of analyzing the experimental results until the very edge of the tube, thus coinciding the maximum level of strains provided by ARGUS<sup>®</sup> with fracture.

Finally, Fig. 4 depicts the numerical evolution of equivalent strain versus average stress triaxiality in the multi-stage tube expansion process by SPIF versus the conventional tube-end expansion. This former numerical evolution corresponding to the average stress triaxiality exposed in [17] ends in levels of triaxiality below 0.2 and would be suitable for explaining the level of equivalent strain attained in the SPIF process. In addition to that, the Mises iso-equivalent fracture elliptical locus  $\bar{\epsilon} = 1.17$  (horizontal dotted line in Fig. 4) that corresponds to the experimental principal strains at fracture in SPIF established the level of strain at which fracture must be actually attained. As can be seen, this level of equivalent strain at fracture is consistent with the end of the evolution of the equivalent strain versus the average stress triaxiality within the triaxiality space, thus providing an alternative explanation for the enhancement of formability in the multi-stage tube by SPIF above the conventional FFL that had been addressed in previous work [13].

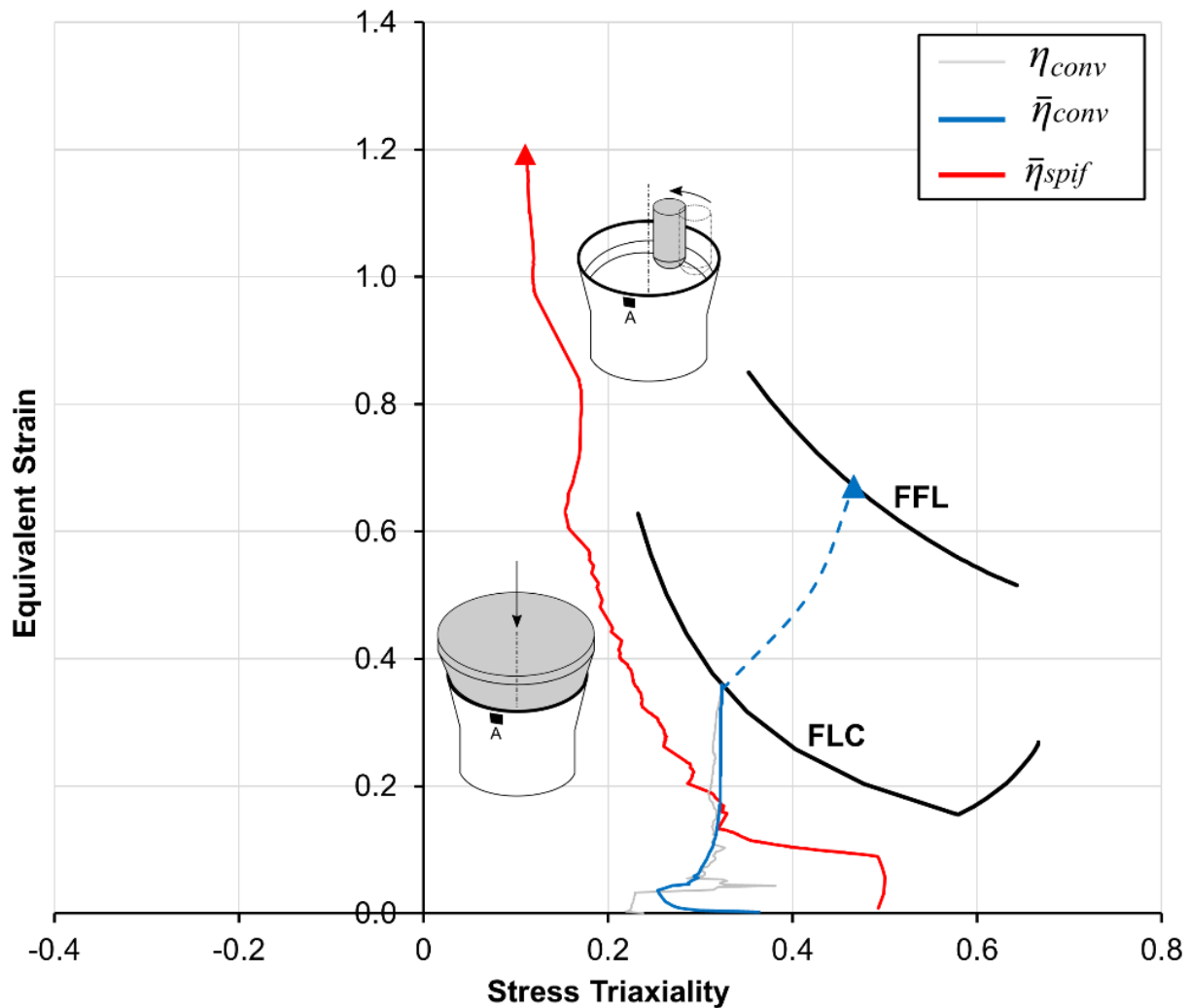


**Figure 4.** Formability analysis in the triaxiality space: numerical evolution of equivalent strain versus average stress triaxiality in multi-stage SPIF and experimental path in conventional expansion

In this regard, 2 overall results can be drawn: (i) the levels of average stress triaxiality attained in the conventional tube expansion (around 0.45) is well above the level attained in the incremental tube expansion (around 0.15). As suggested in [17], this difference results in a greater resistance to accumulate damage in ISF than in conventional forming, resulting in higher levels of equivalent strain to reach ductile fracture, and (ii) results also show a near coincidence of the instantaneous and the average stress-triaxiality evolutions ( $\eta \cong \bar{\eta}$ ) in the conventional process. This result is compatible with the application of McClintock's ductile damage criterion [15] for assessing the onset of failure by fracture in conventional sheet metal forming processes [3]. This latter result ratifies the validity of this overall approach for both the non-proportional paths observed in SPIF of tubes and the near proportional paths attained in conventional tube-end expansion.

## Conclusions

This research discussed a new framework of analysis based in the concept of average stress triaxiality for the analysis of formability and failure in non-proportional tube-end forming processes such as the multi-stage tube expansion process by SPIF, which demonstrated to be also valid for conventional forming. This analysis combines numerical modeling and experimentation, that allow the numerical assessment of the strain paths within the triaxiality space for successfully explaining the enhancement of formability above the conventional fracture forming limit.

The use of effective strain versus stress triaxiality evolutions based on average stress triaxiality to ensure the compatibility with the FFL in tube expansion by SPIF is reasonable due to the cyclically

plastic evolution from shearing to biaxial stretching of a certain deformed tube location as the tool approaches, contacts and moves away from this location of analysis during its trajectory.

This vision has also demonstrated to be compatible with the use of conventional stress-triaxiality instead of its integral form (i.e. average stress-triaxiality) in processes presenting near proportional loading paths such as the case of conventional tube-end expansion, justifying the successful utilization of McClintock's fracture criterion for assessing fracture in conventional forming.

### Acknowledgments

The authors would like to acknowledge the funding received through the Major Grant with reference no. US-1263138 US/JUNTA/FEDER\_UE within the research framework "Proyectos I+D+i FEDER Andalucía 2014-2020".

### References

- [1] G. Centeno, M.B. Silva, L.M. Alves, C. Vallellano, P.A.F. Martins, Towards the characterization of fracture in thin-walled tube forming, *Int. J. Mech. Sci.* 119 (2016) 12–22. <https://doi.org/10.1016/j.ijmecsci.2016.10.001>.
- [2] J.P. Magrinho, G. Centeno, M.B. Silva, C. Vallellano, P.A.F. Martins, On the formability limits of thin-walled tube inversion using different die fillet radii, *Thin-Walled Struct.* 144 (2019). <https://doi.org/10.1016/j.tws.2019.106328>.
- [3] J.P. Magrinho, M.B. Silva, G. Centeno, F. Moedas, C. Vallellano, P.A.F. Martins, On the determination of forming limits in thin-walled tubes, *Int. J. Mech. Sci.* 155 (2019). <https://doi.org/10.1016/j.ijmecsci.2019.03.020>.
- [4] J.P. Magrinho, M.B. Silva, P.A.F. Martins, On the Characterization of Fracture Loci in Thin-Walled Tube Forming, in: *Form. Futur. Miner. Met. Mater. Ser.*, Springer, Cham, 2021: pp. 113–125. [https://doi.org/10.1007/978-3-030-75381-8\\_9](https://doi.org/10.1007/978-3-030-75381-8_9).
- [5] T. McAnulty, J. Jeswiet, M. Doolan, Formability in single point incremental forming: A comparative analysis of the state of the art, *CIRP J. Manuf. Sci. Technol.* 16 (2017) 43–54. <https://doi.org/10.1016/j.cirpj.2016.07.003>.
- [6] X. Zhan, Z. Wang, M. Li, Q. Hu, J. Chen, Investigations on failure-to-fracture mechanism and prediction of forming limit for aluminum alloy incremental forming process, *J. Mater. Process. Technol.* 282 (2020). <https://doi.org/10.1016/j.jmatprotec.2020.116687>.
- [7] J.A. López-Fernández, G. Centeno, A.J. Martínez-Donaire, D. Morales-Palma, C. Vallellano, Stretch-flanging of AA2024-T3 sheet by single-stage SPIF, *Thin-Walled Struct.* 160 (2021). <https://doi.org/10.1016/j.tws.2020.107338>.
- [8] P. Eyckens, S. He, A. Van Bael, P. Van Houtte, J. Dufloy, Forming limit predictions for the serrated strain paths in single point incremental sheet forming, *AIP Conf. Proc.* 908 (2007) 141–146. <https://doi.org/10.1063/1.2740802>.
- [9] M.J. Mirnia, M. Shamsari, Numerical prediction of failure in single point incremental forming using a phenomenological ductile fracture criterion, *J. Mater. Process. Technol.* 244 (2017) 17–43. <https://doi.org/10.1016/j.jmatprotec.2017.01.029>.
- [10] V. Vujovic, A.H. Shabaik, A new workability criterion for ductile metals, *J. Eng. Mater. Technol. Trans. ASME.* 108 (1986) 245–249. <https://doi.org/10.1115/1.3225876>.
- [11] Y. Bao, T. Wierzbicki, On fracture locus in the equivalent strain and stress triaxiality space, *Int. J. Mech. Sci.* 46 (2004) 81–98. <https://doi.org/10.1016/j.ijmecsci.2004.02.006>.

- 
- [12] C. Suntaxi, G. Centeno, M.B. Silva, C. Vallellano, P.A.F. Martins, Tube expansion by single point incremental forming: An experimental and numerical investigation, *Metals (Basel)*. 11 (2021) 1–18. <https://doi.org/10.3390/met11091481>.
  - [13] V.A. Cristino, J.P. Magrinho, G. Centeno, M.B. Silva, P.A.F. Martins, Theory of single point incremental forming of tubes, *J. Mater. Process. Technol.* 287 (2021). <https://doi.org/10.1016/j.jmatprotec.2020.116659>.
  - [14] M.B. Silva, K. Isik, A.E. Tekkaya, A.G. Atkins, P.A.F. Martins, Fracture toughness and failure limits in sheet metal forming, *J. Mater. Process. Technol.* 234 (2016). <https://doi.org/10.1016/j.jmatprotec.2016.03.029>.
  - [15] F.A. McClintock, A Criterion for Ductile Fracture by the Growth of Holes, *J. Appl. Mech.* 35 (1968) 363–371.
  - [16] A.G. Atkins, Fracture in forming, *J. Mater. Process. Technol.* 56 (1996) 609–618. [https://doi.org/10.1016/0924-0136\(95\)01875-1](https://doi.org/10.1016/0924-0136(95)01875-1).
  - [17] A.J. Martínez-Donaire, M. Borrego, D. Morales-Palma, G. Centeno, C. Vallellano, Analysis of the influence of stress triaxiality on formability of hole-flanging by single-stage SPIF, *Int. J. Mech. Sci.* 151 (2019) 76–84. <https://doi.org/10.1016/j.ijmecsci.2018.11.006>.